AD 678 726

FATIGUE CRACK GROWTH IN THREE 180-KSI YIELD STRENGTH STEELS IN AIR AND IN SALT-WATER ENVIRONMENTS

T. W. Crooker, et al

Naval Research Laboratory
Washington, D. C.

26 September 1968

CONTENTS

ABSTRACT

Fatigue crack propagation studies were conducted on three high-strength structural steels: 9Ni-4Co-0.25C, 12Ni maraging, and 18Ni maraging. Each of the steels was heat treated to a yield strength of 180 ksi. Tests were performed in two environments, a "dry" environment consisting of ambient room air and a "wet" environment consisting of 3.5-percent-NaCl salt water.

Relationships for fatigue crack growth rates as a function of the fracture mechanics, stress-intensity factor (K) are developed for each steel, in both environments. The engineering significance of these relationships are then presented in terms of stress levels and flaw sizes relevant to the steels under investigation.

Significant differences were found among the fatigue crack propagation characteristics of the three steels. Response to the "wet" environment varied, depending on the material and the stress-intensity level. The lower toughness steel was less affected by environment, and environmental effects in all the steels diminished with increasing stress-intensity levels. No correlation was observed between fatigue crack propagation behavior in the "wet" environment and the stress-corrosion cracking parameter (K_{Iscc}) obtained on the same materials.

PROBLEM STATUS

This is an interim report on the problem; work is continuing.

AUTHORIZATION

NRL Problems M01-18, M03-01, and F01-17
Projects RR 007-01-46-5420
SF 020-01-01B-12383, and
S-4607-11894

Manuscript submitted June 21, 1968.

FATIGUE CRACK GROWTH IN THREE 180-KSI YIELD STRENGTH STEELS IN AIR AND SALT WATER ENVIRONMENTS

INTRODUCTION

A basic requirement for the fracture-safe application of high-strength structural alloys is the subcritical containment of flaws. Fracture toughness determines the critical flaw size for a given working stress level, and crack growth resistance to fatigue and stress-corrosion determines how rapidly a flaw of critical size can develop in service.

This report discusses fatigue crack growth in three structural steels: 9Ni-4Co-0.25C, 12Ni maraging, and 18Ni maraging. Fatigue crack growth characteristics for a "dry" environment of ambient room air and a "wet" environment of 3.5-percent-NaCl salt water are presented as a function of the fracture mechanics stress-intensity factor (K). Using K as the common analytical parameter, the fatigue results are considered in relation to the fracture toughness (K_{Ic}) and stress-corrosion cracking (K_{Iscc}) characteristics of the steels under investigation. In addition, the structural analysis is reduced to more practical terms by use of stress level and flaw size relationships.

DESCRIPTION OF MATERIALS

Broad spectrum characterization studies conducted at NRL have shown that for structural steels, the 180/200 ksi yield strength (ys) range is a significant transition region for both fracture and fatigue properties. In this region, fracture toughness decreases sharply and fatigue crack growth rates increase sharply. Figure 1 (1) shows fracture toughness characteristics of 1-in.-plate materials as a function of yield strength. This diagram indicates the normal expectancy for fracture toughness in conventionally processed steels and the optimum levels of fracture toughness that can be attained in specially processed steels. A practical engineering index of fracture toughness is obtained by computing the K_{Ic}/σ_{ys} ratio, which normalizes fracture toughness with respect to yield strength. The locus of the unity value of this ratio is indicated in Fig. 1. For 1-in.-plate materials this unity ratio line represents the transition between materials which possess sufficient toughness to fracture in plane stress ($K_{Ic}/\sigma_{ys} > 1.0$) and those materials whose fracture toughness is sufficiently low to fracture in plane strain ($K_{Ic}/\sigma_{ys} < 1.0$). It can be seen from Fig. 1 that this unity ratio line intersects the optimum materials trend line (OMTL) curve near 200 ksi and the normal OMTL expectancy curve at 180 ksi. Thus the critical aspects of this ys region become more apparent. Pellini (1) has noted the critical features of fracture toughness characteristics at the 180-ksi level, and he has also noted the wide range of fracture toughness values measured in various steels at this strength level.

Fatigue crack propagation studies of structural steels performed by the authors are summarized in Fig. 2. This diagram was prepared from the results of characterization studies employing surface-cracked plate bend specimens under strain-controlled cycling (2). Figure 2 shows trends in the rate at which fatigue cracks grow as a function of yield strength under two loading intensities, ys stress (σ_{ys}) and half ys stress ($\sigma_{ys}/2$) and in two environments, ambient room air and 3.5-percent-NaCl salt water. Figure 2 also shows that under optimum service conditions, i.e.,

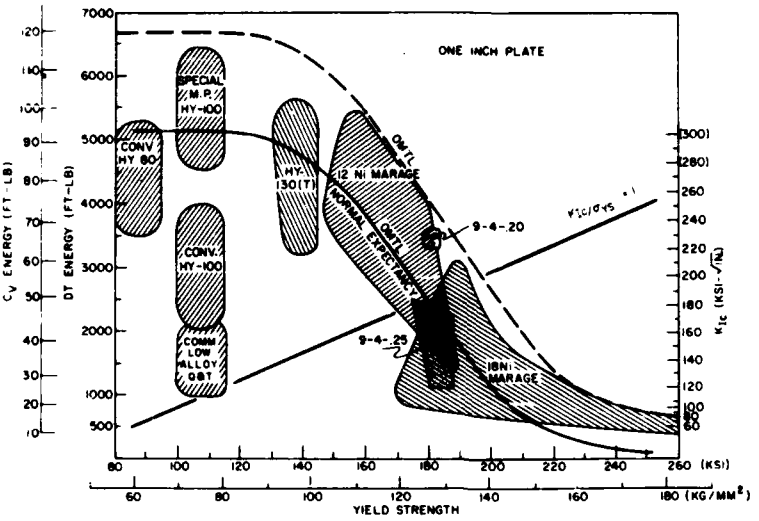

Fig. 1 - Fracture toughness characteristics of structural steels as a function of yield strength (1) indicating the optimum material trend line (OMTL)

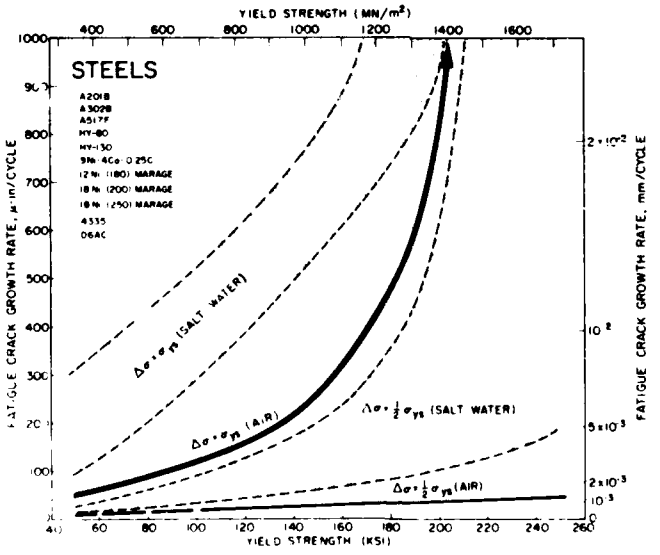

Fig. 2 - Fatigue crack growth rate characteristics of structural steels as a function of yield strength (2)

small flaws, cyclic stresses below $\sigma_{ys}/2$, and a "dry" environment, fatigue crack growth occurs slowly in all steels. Under these conditions, fatigue failures are unlikely except in cases where a flaw of substantial size has gone undetected or in materials of very low fracture toughness where critical flaw sizes may be very small. However, once a departure has been made from these optimum conditions, fatigue cracks tend to grow much more rapidly, especially in higher strength steels.

Surveying the spectrum of data, it can be seen that the 180/200-ksi ys range is critical for fatigue as well as for fracture. An exceedingly broad range of fatigue performance can be noted in this region. Fatigue crack growth rates can vary over more than two orders of magnitude, depending on the material, load intensity, and environment. Also, it can be noted that the ys region above 180/200 ksi is characterized by trends toward very rapid fatigue crack growth.

A detailed description of the materials under investigation is summarized in Tables 1 through 4. A broad range of studies have been performed on these materials by various NRL investigators, and the results have been brought together to serve as background information. Identification of the parent plate is provided by the NRL code number. Minor variations in strength and toughness properties occur among samples taken from a given plate, depending on fracture orientation and heat treatment. The ASTM fracture identification procedure (3) is employed, as illustrated in Fig. 3. Tensile and impact properties given in Table 3 refer to the specific strength level and orientation of the fatigue specimens. However, the fracture mechanics data given in Table 4 refers, in some cases, to other orientations and strength levels as identified.

Table 1
Chemical Compositions

Material	NRL Code	Element (wt %)											
		C	Mn	P	S	Si	Ni	Cr	Mo	Co	V	Ti	Al
9Ni-4Co-0.25C	J15	0.25	0.28	0.006	0.008	0.01	8.31	0.40	0.48	3.78	0.11	-	-
12Ni Maraging	J7	0.007	0.04	0.005	0.007	0.07	11.8	5.12	3.30	-	-	0.24	0.11
18Ni Maraging	K15	0.005	0.07	0.008	0.005	0.01	18.8	-	4.60	8.66	-	0.40	0.24

Table 2
Description of Processing

Material	NRL Code	Rolling Procedure	Heat Treatment
9Ni-4Co-0.25C	J15	Highly Cross-Rolled to 1-in. Thick Plate	Mill: Normalized at 1600°F. 1 Hour, Austenitized at 1500°F. 1 Hour, Oil Quenched, Tempered at 1000°F., Air Cooled
12Ni Maraging	J7	Highly Cross-Rolled to 1-in. Thick Plate	Mill: Solution Annealed at 1500°F; NRL: Aged 20 Hours at 900°F., Air Cooled
18Ni Maraging	K15	Highly Cross-Rolled to 1-in. Thick Plate	Mill: Solution Annealed at 1650°F.; NRL: Aged 3 Hours at 900°F., Air Cooled

Table 3
Tensile and Impact Properties

Material	NRL Code	Fracture Orientation	0.505-in.-Dia. Tension Test Data				Impact Data	
			0.2% ys (ksi)	UTS (ksi)	Elong. (%)	R.A. (%)	C_v at 30°F (ft-lb)	1-in. Dynamic Tear at 30°F (ft-lb)
9Ni-4Co-0.25C	J15	WR	183.2	195.0	17.0	61.0	40	1966
12Ni Maraging	J7	WR	181.5	188.5	14.5	62.3	66	3843
18Ni Maraging	K15	RW	179.9	191.4	14.0	62.2	47	4160

Table 4
Fracture Mechanics Data

Material	NRL Code	Fracture Toughness				Stress-Corrosion Cracking			
		σ_{ys} (ksi)	Fracture Orientation	Corrected K_{Ic} (ksi $\sqrt{in.}$)	NRL Investigator	σ_{ys} (ksi)	Fracture Orientation	K_{Iscc} (ksi $\sqrt{in.}$)	NRL Investigator
9Ni-4Co-0.25C	J15	183	RW	155	C.N. Freed	183	RW	100	G. Sandoz
		183	WR	153	C.N. Freed				
		183	WT	159	H.L. Smith				
12Ni Maraging	J7	176	WR	249	H.L. Smith	181	WT	70	G. Sandoz
		176	WT	246	H.L. Smith	181	RT	80	G. Sandoz
18Ni Maraging	K15	197	RW*	231	H.L. Smith	197	RW	104	G. Sandoz
		205	WR	194	H.L. Smith				

EXPERIMENTAL PROCEDURE

Fatigue crack propagation tests were performed using single-edge-notched (SEN) specimens cycled zero-to-tension in cantilever bending. A detail drawing of the fatigue specimen is shown in Fig. 4. The test section has nominal dimensions of 2.5 in. wide and 0.5 in. thick. The net thickness is reduced to 0.45 in. by side-grooving, which acts to suppress shear lip formation and promote a straight crack front. The edge-notch is nominally 0.5 in. deep, and fatigue crack propagation is allowed to extend the flaw to a maximum total depth of 1.5 in. Measurements of fatigue crack length are performed by a slide-mounted optical micrometer focused on the root surface of one side-groove.

Special techniques aid optical observation of the fatigue crack tip. Tool marks are obliterated from the side-groove surface by applying a light sandblast, which causes reflected light to be diffused, thus eliminating glare. During fatigue testing, an intense light is focused on the area of the crack tip, and a dark red optical filter is placed in front of the 32-mm-focal-length objective lens of the optical micrometer. These procedures produce a sharp, clear view of the fatigue crack tip. For a test specimen as shown in Fig. 4, the combination of test section thickness and side-groove results in a straight crack front, thereby allowing accurate measurements from surface observations.

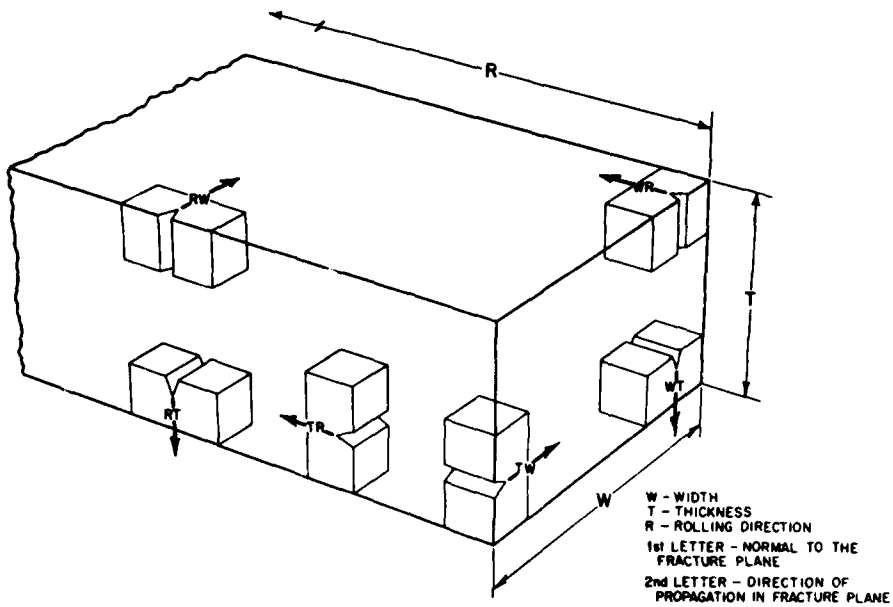

Fig. 3 - ASTM identification procedure for fractures in rolled plate (3)

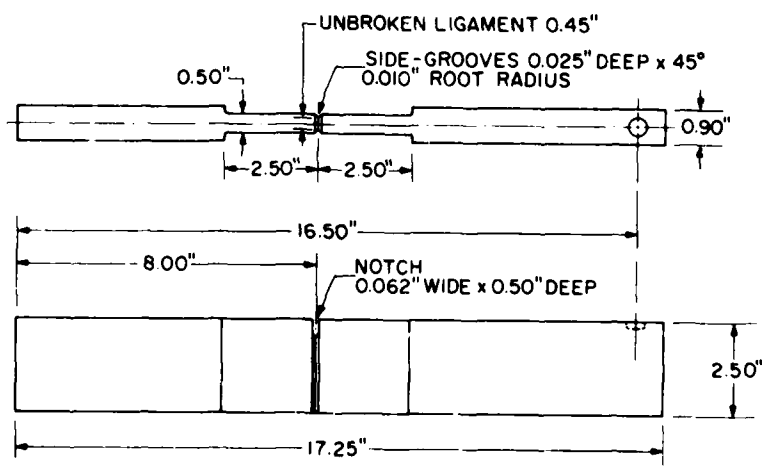

Fig. 4 - NRL single-edge-notched (SEN) cantilever fatigue specimen with side-grooves

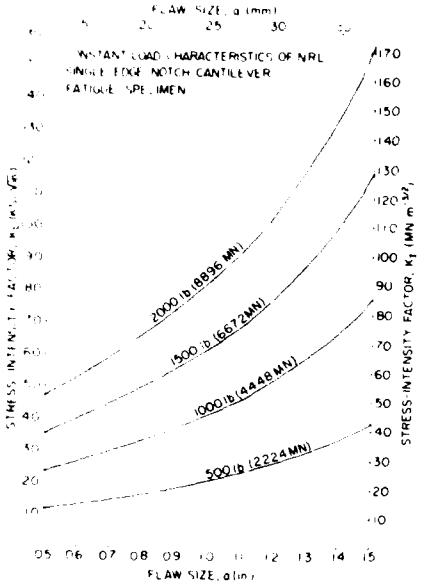

Fig. 5 - Stress-intensity (K) characteristics of the SEN fatigue specimen as a function of flaw size (a) for various constant loads. The curves were calculated from Kies' equation (4).

The fatigue crack propagation tests were run under constant load, zero-to-tension at a frequency of 5 cpm. As the crack propagates through the test section, the stress-intensity factor range (ΔK) increases, producing a range of crack growth rates for study. The stress-intensity characteristics of the fatigue specimen are illustrated in Fig. 5, where the relationship between stress-intensity factor (K) and flaw size (a) is shown for several load values. Flaw size is defined as total crack depth measured from the specimen edge and includes the nominal 0.5-in. notch. The stress-intensity curves in Fig. 5 were computed from the equation of Kies (4).

The "wet" environment studies were performed by placing a polyurethane cell around the test section. Distilled water containing 3.5-percent NaCl was continuously pumped through the cell from a reservoir. The salt water was filtered and aerated on a continuous flow basis. The cell contained a plexiglas window for crack observation. Periodic cleaning of the side-groove surface was required to remove corrosion deposits.

Specimens were cycled until a maximum flaw size of 1.5 in. was grown or until failure occurred. Failure is defined as brittle fracture or gross yielding. Continuous measurements of moment arm deflection displayed on a strip recorder indicated the onset of gross yielding.

RESULTS AND DISCUSSION

Crack Growth Rate Analysis

A crack growth rate analysis provides the most general comparative basis for characterizing the fatigue behavior of materials. In addition, a crack growth rate analysis serves as a transitional function between laboratory specimen data and crack growth in structures. An empirical correlation between the fatigue crack growth rate (da/dN) and the fracture mechanics, stress-intensity factor range (ΔK) was originally proposed by Paris (5), and it has now been adopted by many investigators in the field. The chief benefit of this approach is that both parameters employed in the correlation

are not restricted to the specific test conditions and may be interpreted for a wide variety structures provided the necessary conditions for a fracture mechanics analysis prevail. Basically, these conditions are an accurate knowledge of flaw size and shape, an accurate stress analysis, and assurance that gross yielding has not occurred.

Growth rate data for the three steels under investigation are shown in Figs. 6 through 8, and summarized in Figs. 9 and 10. These figures are log-log plots of da/dN versus ΔK. The open symbols denote data from tests conducted in the "dry," room air environment, and the closed symbols denote data from the "wet," 3.5-percent NaCl salt water environment. The threshold stress-intensity level, above which stress-corrosion cracking (K_{Iscc}) can occur, is indicated on these figures for each steel. The significance of the K_{Iscc} parameter, developed by Brown, is discussed in Ref. 6.

The following observations pertain to the fatigue crack growth rate data presented in Figs. 6 through 8. The growth rate data for all three steels in air follow power-law relationships of the form $da/dN = C(\Delta K)^m$. The value of the exponent m is 2.3 for the two maraging steels and 4.0 for the 9Ni-4Co-0.25C steel. Although the mathematical form of the relationships is the same for each steel, significant differences are apparent among the three curves. These data do not conform to a common crack propagation law, except perhaps in very broad terms; and the crack propagation characteristics of 180-ksi ys steels must be considered on an individual basis.

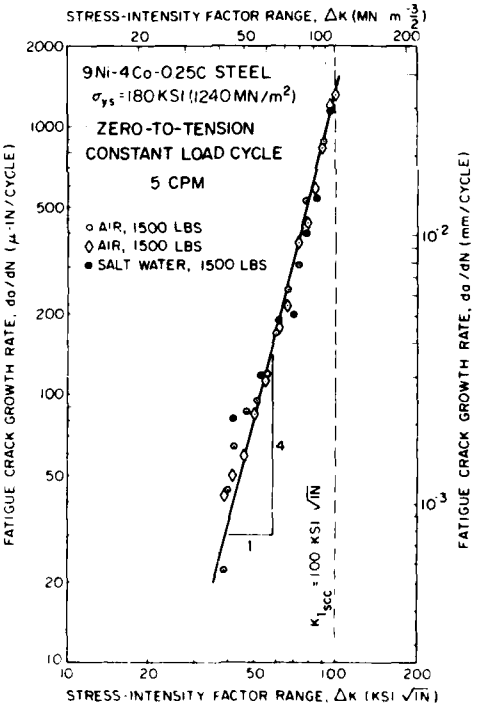

Fig. 6 - Log-log plot of fatigue crack growth rate (da/dN) versus stress-intensity factor range (ΔK) for 9Ni-4Co-0.25C steel. The open symbols denote air environment data and the closed symbols denote salt water environment data. The K_{Iscc} stress-intensity level of 100 ksi$\sqrt{in}$, is indicated by the dashed line.

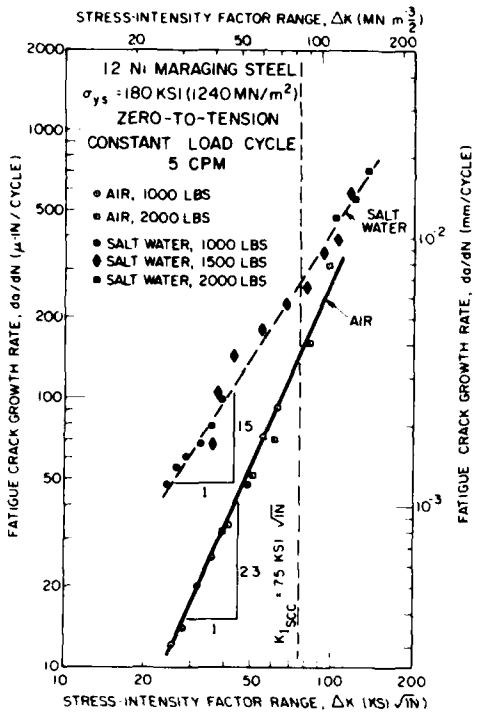

Fig. 7 - Log-log plot of fatigue crack growth rate (da/dN) versus stress-intensity factor range (ΔK) for 12Ni maraging steel. The K_{Iscc} level is 75 ksi$\sqrt{in.}$

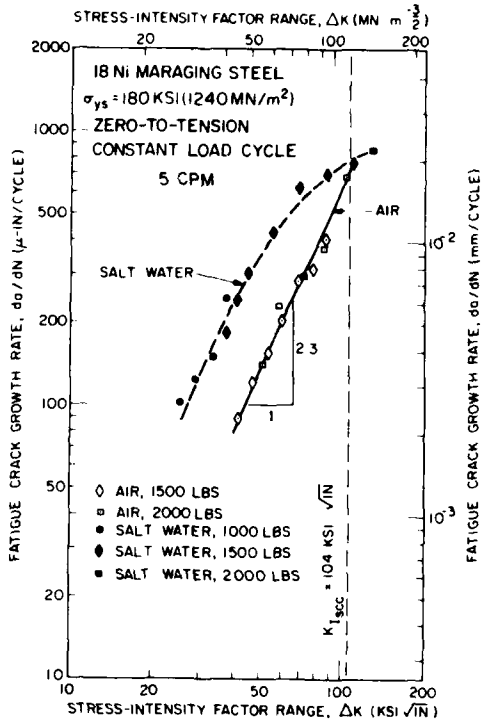

Fig. 8 - Log-log plot of fatigue crack growth rate (da/dN) versus stress-intensity factor range (ΔK) for 18Ni maraging steel. The K_{Iscc} level is 104 ksi$\sqrt{in.}$

The fatigue crack growth rate data for the steels in salt water are also included in Figs. 6 through 8 and are summarized in Fig. 10. It is common knowledge that the presence of a salt water environment can accelerate fatigue crack growth. The purpose of this study was to determine the magnitude of these accelerations and to assess the usefulness of the static K_{Iscc} parameter for predicting the salt water, fatigue crack growth behavior.

The response of the three steels to salt water at the 5 cpm loading rate varied, depending on the alloy and the stress-intensity. In each case, however, the greatest acceleration in growth rates occurred at low ΔK levels, below 40 ksi$\sqrt{in.}$, which was less than half the K_{Iscc} value. Also, in each case the acceleration in growth rates decreased as the ΔK level increased. In all cases the "wet" environment growth rate curves tended toward convergence with the "dry" environment growth rate curves at higher ΔK levels. The maximum environmental effects on growth rates were less than an order of magnitude in all cases. Among the three steels under investigation, 9Ni-4Co-0.25C exhibited the least response to the salt water environment.

There was no apparent correlation between these data and the K_{Iscc} parameter. This is attributed to the fact that stress-corrosion cracking occurs very slowly in these steels. Fatigue loading at 5 cpm does not allow sufficient time for this crack propagation mechanism to exert a strong influence on crack growth rates. In contrast, where stress-corrosion cracks propagate much more rapidly in titanium alloys than in steels, several

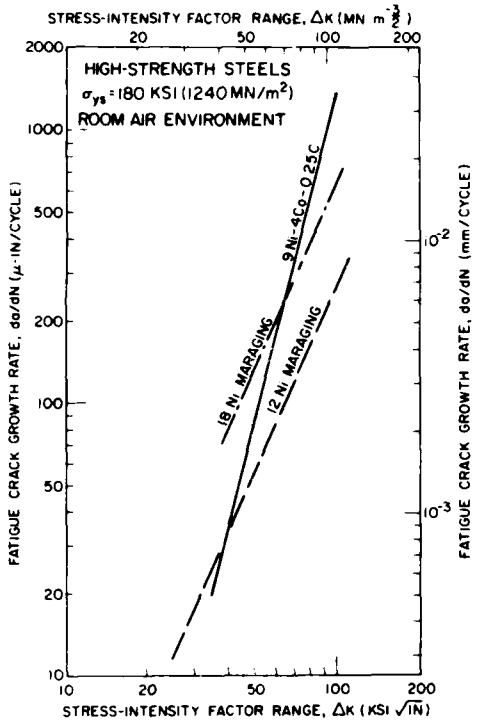

Fig. 9 - Summary of air environment fatigue crack growth rate curves

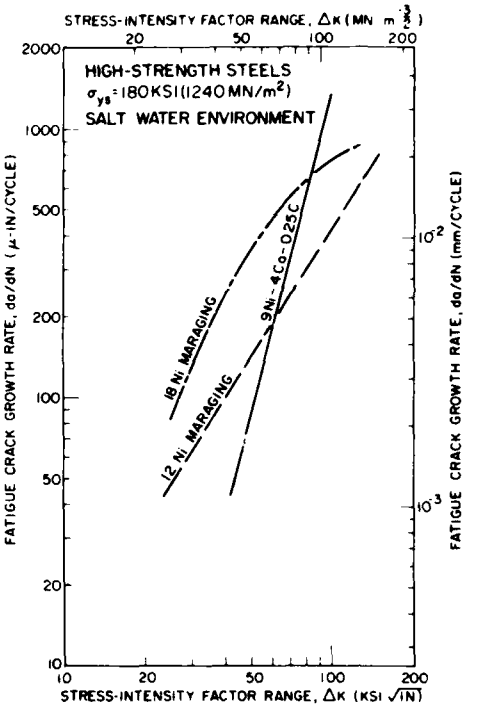

Fig. 10 - Summary of salt-water environment fatigue crack growth rate curves

investigators (7,8) have proposed that K_{Iscc} can serve as an index of salt-water fatigue behavior by indicating the onset of rapid fatigue crack growth.

All samples of the 9Ni-4Co-0.25C steel under investigation, both in air and in salt water, developed very rapid rates of fatigue crack growth at a ΔK level of approximately 100 ksi $\sqrt{\text{in}}$. This happens to coincide with the value of the K_{Iscc} parameter for this steel, which would suggest that environmental cracking played a role in this rapid crack propagation behavior. A separate study was made of this phenomenon using electron fractography, and no evidence was found to indicate that environmental cracking was significant (9). The microfracture modes in the fast growth rate regions consisted exclusively of shallow dimples. No cleavage or quasi-cleavage, usually associated with environmental cracking, was observed. Therefore, it was concluded that this behavior was related to fracture toughness rather than environmental cracking.

Stress Level-Flaw Size Relationships for Fatigue

Fatigue crack growth rate data, as a function of stress-intensity, can be restated in terms of stress level and flaw size relationships. The stress-intensity factor (K) is proportional to the product of stress (σ) times the square root of flaw size ($\sqrt{a}$); the exact expression being dependent on the shape and the dimensions of the structure. Figures 11 and 12 are linear plots of fatigue crack growth rate (da/dN) versus flaw depth (a). The conditions under which these curves apply is an axial-loaded, surface-cracked plate containing a semicircular flaw that has been studied extensively by Tiffany (10). Two

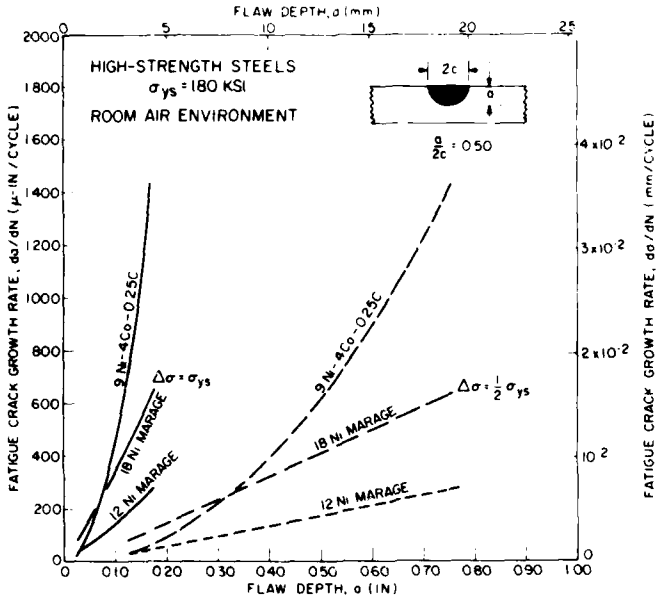

Fig. 11 - Linear plot of fatigue crack growth rate (da/dN) as a function of flaw depth (a) in air for the three 180-ksi steels. The curves are based on stress-intensity factors for an axial-loaded surface-cracked plate (10), and refer to a semicircular flaw (a/2c = 0.50) at two cyclic stress levels, σ_{ys} and $\sigma_{ys}/2$.

groups of curves are shown in each figure; one group refers to cyclic stress levels of 0 to σ_{ys} ($\Delta\sigma = \sigma_{ys}$), and the other group refers to cyclic stress levels 0 to $\sigma_{ys}/2$ ($\Delta\sigma = \sigma_{ys}/2$). Figure 11 shows air environment curves and Fig. 12 shows salt water environment curves. The initiation of each curve corresponds to a ΔK level of 40 ksi $\sqrt{\text{in.}}$ and the termination corresponds to a ΔK level of 100 ksi $\sqrt{\text{in.}}$

The curves present a graphic illustration of the ability of these steels to contain flaws subcritically, as measured in terms of cyclic stress levels and flaw sizes. Although these curves are not complete, in the sense that the fatigue crack growth is not traced all the way to the critical stress-intensity (K_{Ic}), it can be seen that the flaw sizes for steels at the 180-ksi ys level are relatively small. It can also be seen that significant differences exist among the fatigue characteristics of these steels. Although the salt water environment curves are displaced to higher growth rates than the air environment curves, the relative order of the curves is not significantly changed. Viewed on the basis of these plots, 12Ni maraging steel clearly emerges as possessing the most favorable fatigue crack growth resistance of the three 180-ksi ys steels.

The results of this study should be viewed in relation to the following qualifications. With the exception of the 9Ni-4Co-0.25C steel, fatigue crack growth was not pursued all the way to critical fracture conditions. To do so, within the framework of linear elastic fracture mechanics, larger test section sizes are required for the high toughness maraging steels studied. Therefore, the overall fatigue performance data must be considered as incomplete for the maraging steels. In addition, the "wet" environment data and their

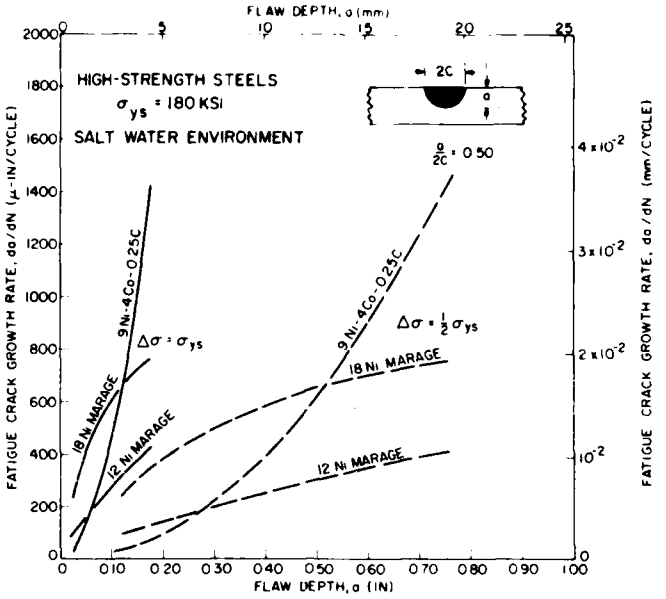

Fig. 12 - Linear plot of fatigue crack growth rate (da/dN) as a function of flaw depth (a) in salt water for the three 180-ksi ys steels. The curves are based on stress-intensity factors for an axial-loaded surface-cracked plate (10), and refer to a semicircular flaw (a/2c = 0.50) at two cyclic stress levels, σ_{ys} and $\sigma_{ys}/2$.

relationship to K_{Iscc} must be considered as potentially sensitive to loading frequency and fracture orientation. These aspects warrant further study.

SUMMARY AND CONCLUSIONS

Fatigue crack propagation studies were conducted on three 180-ksi ys steels; 9Ni-4Co-0.25C, 12Ni maraging, and 18Ni maraging. Tests using single-edge-notched (SEN) cantilever specimens cycled zero-to-tension were conducted in a "dry" environment of ambient room air and a "wet" environment of 3.5-percent NaCl salt water. Results were analyzed in terms of the fracture mechanics, stress-intensity factor (K). The following conclusions have been reached from this study:

1. For three steels with the same 180-ksi ys level, significant differences were observed among their fatigue crack growth rate characteristics, measured as a function of the stress-intensity factor (K).

2. Fatigue crack growth in all three steels was accelerated by the "wet" environment, but only to a limited extent. The greatest accelerations were of less than an order of magnitude and occurred under low stress-intensity (ΔK = 40 ksi$\sqrt{\text{in.}}$). Convergence of the "wet" and "dry" growth-rate curves occurred at higher stress-intensity (ΔK = 100 ksi$\sqrt{\text{in.}}$).

3. No correlation was observed between "wet" fatigue crack growth behavior in these steels and the stress-corrosion cracking parameter (K_{Iscc}) obtained on the same materials. This lack of correspondence between the two modes of subcritical flaw growth

is attributed to the fact that, although these steels are susceptible to stress-corrosion cracking, long periods of time under static load are required to propagate stress-corrosion cracks. Cyclic loading at 5 cpm does not provide sufficient time for stress-corrosion cracking to exert a strong influence on fatigue crack growth in these steels.

ACKNOWLEDGMENTS

The authors wish to acknowledge the work of Mr. R.J. Hicks who performed the fatigue tests. The authors are also grateful for the continued financial support of this work by the Office of Naval Research, the Naval Ship Systems Command, and the Deep Submergence Systems Project.

REFERENCES

1. Pellini, W.S., "Advances in Fracture Toughness Characterization Procedures and in Quantitative Interpretations to Fracture-Safe Design for Structural Steels," NRL Report 6713, Apr. 3, 1968

2. Crooker, T.W., and Lange, E.A., "Low Cycle Fatigue Crack Propagation Resistance of Materials for Large Welded Structures," p. 94 in "Fatigue Crack Propagation," ASTM STP 415, 1967

3. Anonymous, "The Slow Growth and Rapid Propagation of Cracks," Mater. Res. Std. 1(No. 5):389 (May 1961)

4. Kies, J.A., Smith, H.L., Romine, H.E., and Bernstein, H., "Fracture Testing of Weldments," p. 328 in "Fracture Toughness Testing and Its Applications," ASTM STP 381, 1965

5. Paris, P.C., "The Fracture Mechanics Approach to Fatigue," p. 107 in "Fatigue - An Interdisciplinary Approach, Proceedings Tenth Sagamore Army Materials Research Conference," Aug. 13-16, 1963; Syracuse Univ. 1964

6. Brown, B.F., "A New Stress-Corrosion Cracking Test for High-Strength Alloys," Mater. Res. Std. 6(No. 3):129 (Mar. 1966)

7. Piper, D.E., Smith, S.H., and Carter, R.V., "Corrosion Fatigue and Stress-Corrosion Cracking in Aqueous Environments," Boeing Company Document D6-60067, Renton, Wash., Mar. 1967

8. Crooker, T.W., and Lange, E.A., "Corrosion Crack Propagation in Ti-6Al-4V Under Static and Cyclic Loading," Report of NRL Progress, p. 25, Feb. 1968

9. Crooker, T.W., Cooley, L.A., Lange, E.A., and Freed, C.N., "Subcritical Flaw Growth in 9Ni-4Co-0.25C Steel - A Fatigue and Fractographic Investigation and Its Relationship to Plane Strain Fracture Toughness," NRL Report 6698, May 1, 1968

10. Tiffany, C.F., and Masters, J.N., "Applied Fracture Mechanics," p. 249 in "Fracture Toughness Testing and Its Applications," ASTM STP 381, 1965

Security Classification

DOCUMENT CONTROL DATA - R & D

(Security classification of title, body of abstract and indexing annotation must be entered when the overall report is classified)

1 ORIGINATING ACTIVITY (Corporate author)	2a. REPORT SECURITY CLASSIFICATION
Naval Research Laboratory Washington, D.C., 20390	Unclassified
	2b. GROUP

3 REPORT TITLE

FATIGUE CRACK GROWTH IN THREE 180-KSI YIELD STRENGTH STEELS IN AIR AND SALT WATER ENVIRONMENTS

4 DESCRIPTIVE NOTES (Type of report and inclusive dates)

An interim report on a continuing problem.

5 AUTHOR(S) (First name, middle initial, last name)

T.W. Crooker and E.A. Lange

6 REPORT DATE	7a. TOTAL NO. OF PAGES	7b. NO. OF REFS
September 26, 1968	16	10

8a. CONTRACT OR GRANT NO	9a. ORIGINATOR'S REPORT NUMBER(S)
NRL Problem M01-18, M03-01, and b. PROJECT NO. F01-17 RR 007-01-46-5420, SF 020-01-01B- c. 12383, and S-4607-11894 d.	NRL Report 6761
	9b. OTHER REPORT NO(S) (Any other numbers that may be assigned this report)

10. DISTRIBUTION STATEMENT

This document has been approved for public release and sale; its distribution is unlimited.

11. SUPPLEMENTARY NOTES	12. SPONSORING MILITARY ACTIVITY
	Dept. of the Navy (Office of Naval Research) Washington, D.C., 20360

13. ABSTRACT

Fatigue crack propagation studies were conducted on three high-strength structural steels: 9Ni-4Co-0.25C, 12Ni maraging, and 18Ni maraging. Each of the steels was heat treated to a yield strength of 180 ksi. Tests were performed in two environments, a "dry" environment consisting of ambient room air and a "wet" environment consisting of 3.5-percent-NaCl salt water.

Relationships for fatigue crack growth rates as a function of the fracture mechanics, stress-intensity factor (K) are developed for each steel, in both environments. The engineering significance of these relationships are then presented in terms of stress levels and flaw sizes relevant to the steels under investigation.

Significant differences were found among the fatigue crack propagation characteristics of the three steels. Response to the "wet" environment varied, depending on the material and the stress-intensity level. The lower toughness steel was less affected by environment, and environmental effects in all the steels diminished with increasing stress-intensity levels. No correlation was observed between fatigue crack propagation behavior in the "wet" environment and the stress-corrosion cracking parameter (K_{Iscc}) obtained on the same materials.

DD FORM 1 NOV 68 1473 (PAGE 1)

S/N 0101-807-6801

Security Classification

14 KEY WORDS	LINK A		LINK B		LINK C	
	ROLE	WT	ROLE	WT	ROLE	WT
High-strength structural alloys Subcritical flaws Fracture toughness Stress-corrosion cracking Fatigue crack growth rate Dry environment Salt-water environment Fracture mechanics, stress-intensity factor 180-ksi yield strength steels Cyclic loading Growth rate - flaw size diagram						